Article ID

DnCNN-RM: An Adaptive SAR Image Denoising Algorithm Based on Residual Networks

OU Hai-ning[1], LI Chang-di[2], ZENG Rui-bin[1,*], WU Yan-feng[3], LIU Jia-ning[2], CHENG Peng[2]

([1]*Department of Automation Engineering, Meizhouwan Vocational Technology College, Putian, 351100*

[2]*Suzhou Duty Ratio Information Technology Co., Ltd., Suzhou, 215000*

[3]*School of Computer Science and Technology, University of Science and Technology of China, Hefei, 230000*)

** Corresponding Author, E-mail: zengruibin19@mails.ucas.ac.cn*

Abstract: In the field of image processing, the analysis of Synthetic Aperture Radar (SAR) imagery is crucial due to its broad range of applications. However, SAR images are often affected by coherent speckle noise, which severely degrades image quality. Traditional denoising methods, typically based on filter-based techniques, often face challenges in terms of inefficiency and limited adaptability. To address these limitations, this study proposes a novel SAR image denoising algorithm based on an enhanced residual network architecture, aimed at improving the utility of SAR imagery in complex electromagnetic environments. The proposed algorithm integrates residual network modules, which directly process the noisy input images to generate denoised outputs. This approach not only reduces computational complexity but also mitigates the difficulties associated with model training. By combining the Transformer module with the residual block, the algorithm enhances the network's ability to extract global features, offering superior feature extraction capabilities compared to CNN-based residual modules. Furthermore, the algorithm incorporates the adaptive activation function Meta-ACON, which dynamically adjusts the activation patterns of neurons, thus improving the network's feature extraction efficiency. The effectiveness of the proposed denoising method was empirically validated using real SAR images from the RSOD dataset. The algorithm demonstrated exceptional performance in terms of EPI, SSIM, and ENL, while significantly improving PSNR. Compared to both traditional and deep learning-based algorithms, the PSNR performance was enhanced by over twofold. Furthermore, evaluation on the MSTAR SAR dataset demonstrated a PSNR of 25.2021, thereby substantiating the algorithm's robustness and applicability in SAR denoising tasks. These results indicate that the proposed algorithm effectively reduces speckle noise while preserving critical features in SAR imagery, thereby enhancing its quality and usability in practical scenarios.

Key words: SAR images, Image denoising, Residual networks, Adaptive activation function

CLC number: **Document code**:

收稿日期： ；修订日期：
基金项目：无

DnCNN-RM：基于残差网络的自适应合成孔径雷达图像去噪算法

欧海宁[1]，李长頔[2]，曾瑞彬[1,*]，吴言枫[3]，刘佳宁[2]，程鹏[2]

（[1]湄洲湾职业技术学院 自动化工程系，福建 莆田，351100
[2]苏州占空比信息科技有限公司， 江苏 苏州，215000
[3]中国科学技术大学，计算机科学与技术学院，安徽 合肥，230000）

摘要：在图像处理领域，合成孔径雷达（SAR）图像的分析由于其广泛的应用而具有重要意义。然而，这些图像常常受到相干斑噪声的干扰，显著降低了图像质量。传统的去噪方法，通常基于滤波器技术，往往存在效率低下和适应性差的局限性。为了克服这些不足，本文提出了一种基于增强残差网络架构的 SAR 图像去噪算法，旨在提升 SAR 图像在复杂电磁环境中的应用效果。该算法结合了残差网络模块，直接对含噪输入图像进行处理，生成去噪输出。这种方法不仅有效降低了计算复杂度，还缓解了模型训练过程中遇到的困难。通过将 Transformer 模块与残差块结合，该算法提高了网络对全局特征的提取能力，相较于基于卷积神经网络（CNN）的残差模块，具有更强的特征提取能力。此外，算法引入了自适应激活函数 Meta-ACON，能够动态调整神经元的激活模式，从而进一步提升了网络在特征提取上的效率。通过在 RSOD 数据集上的实验证明，所提出的去噪方法在 EPI、SSIM 和 ENL 等指标上表现出色，同时在 PSNR 方面也取得了显著的提升。与传统的去噪算法及深度学习算法相比，该算法的 PSNR 性能提高了两倍以上。进一步在 MSTAR SAR 数据集上的测试，得到了 PSNR 值为 25.2021，验证了该算法在 SAR 去噪领域的良好泛化性。这些结果表明，所提出的算法 s 不仅能够有效降低相干斑噪声，还能有效保留 SAR 图像中的关键信息特征，从而在实际应用中显著提高图像质量和可用性。

关键词：合成孔径雷达图像、图像去噪、残差网络、自适应激活函数

1 Introduction

Synthetic Aperture Radar (SAR), as a form of microwave radar, is distinguished by its ability to provide high-resolution imaging. Unlike conventional radar systems, which are constrained by the fixed aperture size, SAR utilizes a synthetic aperture mechanism to enhance imaging resolution [1-3]. However, SAR images are often affected by coherent speckle noise, a form of artifact generated by the coherent nature of the imaging process [4]. This noise manifests as granular patterns within the image, reducing the signal-to-noise ratio (SNR) and degrading image quality [5]. Such degradation presents significant challenges for subsequent analysis and interpretation tasks. Therefore, the development of effective algorithms for reducing coherent speckle noise is crucial to improving SAR image processing [6-7].

In critical tasks of SAR image processing, including target detection, image reconstruction, and denoising, numerous technical challenges persist. Firstly, effectively extracting discriminative features from high-dimensional SAR data, particularly in scenarios with limited data, remains an unresolved issue. In recent years, deep learning-based multimodal approaches have gradually become a research focus [8]. These approaches primarily enhance target detection and classification accuracy by integrating different types of remote sensing data. Furthermore, cross-modal data fusion has demonstrated high accuracy in tasks such as target detection, classification, and change detection. However, due to the distinct physical properties of different types of remote sensing data, effectively performing cross-modal data fusion while maintaining the model's generalization capability remains a significant research challenge. Zhang et al. proposed a deep learning-based cross-modal image fusion method, which achieves efficient integration of data from

multiple sensors through the joint training of several network models, significantly enhancing the model's applicability and stability across various scenarios [9]. In real-time monitoring and emergency response, the rapid processing of large-scale SAR data while maintaining high processing accuracy remains an urgent challenge. Zhao et al. proposed a solution based on lightweight convolutional neural networks (CNNs), which, by incorporating pruning and quantization techniques, significantly reduce computational complexity while ensuring high denoising and detection performance [10].

Coherent speckle noise, in contrast to other types of noise, typically leads to intense local fluctuations and dramatic changes in signal phase and amplitude, making it distinct from other forms of noise. Although the impact of speckle noise is relatively minimal in low-reflectivity regions, it significantly distorts the details in high-reflectivity areas. This necessitates denoising methods that account for both the spatial variability of the noise and the local features of the image.

Traditional denoising methods often struggle to achieve an optimal balance between noise removal and detail preservation. In recent years, deep learning methods, such as CNNs and generative adversarial networks (GANs), have made significant advancements in SAR image denoising tasks. For example, Zhu et al. proposed a deep convolutional neural network-based denoising algorithm that effectively removes speckle noise while preserving image details [11]. Liu et al. employed multi-scale convolutional networks and multi-view fusion strategies to more effectively address the diversity and complexity of SAR images [12]. Additionally, Li et al. introduced a denoising strategy that combines adaptive filtering with deep learning methods, which dynamically adjusts denoising strength based on the local characteristics of the image, achieving favorable denoising results [13].

In this paper, we propose a deep learning-based SAR image denoising algorithm, which incorporates residual units. Given the distinct nature of coherent speckle noise—both in terms of its origin and distribution—our proposed denoising method is specifically designed to target this type of noise, with the goal of enhancing the quality of SAR images. The main contributions of this work are as follows:

(1) A residual network module is introduced, augmented with a Transformer architecture, to generate new residual blocks. This modification improves the algorithm's ability to extract global features from SAR images, thereby preserving essential global information.

(2) We incorporate an adaptive activation function, Meta-ACON, into the DnCNN network. By training the switching factors in the custom-designed CNN network, Meta-ACON adaptively eliminates irrelevant features, thus enhancing feature extraction efficiency.

(3) The proposed SAR image denoising algorithm, DnCNN-RM, is evaluated on the MSTAR SAR image dataset to validate its generalization ability. The results demonstrate the effectiveness and practicality of the algorithm, as well as the feasibility of simulating coherent speckle noise.

2 Method

2.1 Residual Network Mechanism

The structure of the residual block in the Deep Residual Network (DRN) is illustrated in Fig. 1. Let the initial input features be denoted by x, and the desired output of the DRN by $H(x)$. In this context, the learning objective can be reformulated as learning a residual mapping, where the network is tasked with learning only the difference between the input and output, rather than the entire transformation. As the residual approaches zero, the output of the network approximates the input x, making the residual function equivalent to the identity mapping. As a result, the original function $H(x)$ is transformed, with the identity mapping of x effectively being passed through to the output.

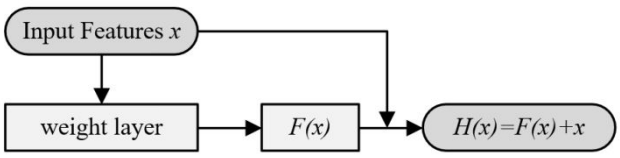

Fig. 1 Residual unit module structure diagram

2.2 Transformer

The Transformer model, introduced by Vaswani et al., has revolutionized the field of natural language processing (NLP) and extended its impact to other domains such as computer vision and speech processing. Unlike traditional recurrent neural networks (RNNs) and CNNs, the Transformer leverages a self-attention mechanism to process input sequences in parallel, rather than sequentially. This parallelization significantly improves both training efficiency and model scalability, especially in tasks requiring long-range dependencies.

At the core of the Transformer architecture is the self-attention mechanism, which allows the model to weigh the importance of each element in the input sequence relative to others, irrespective of their distance in the sequence. The Transformer employs multi-head attention, enabling the model to attend to different parts of the sequence simultaneously, capturing various semantic relationships. The encoder-decoder structure, with layers of attention and feed-forward networks, allows the model to encode complex patterns and generate meaningful output representations.

2.3 Meta-ACON

ACON is designed to adaptively activate neurons [14]. The switching factor, denoted as β, serves as a hyperparameter that governs the activation of neurons. When β approaches 0, ACON displays reduced nonlinearity, leading to smaller weights for the corresponding neuron. As a result, neural networks can efficiently extract features, minimizing the extraction of redundant and irrelevant information.

ACON employs $S_\beta(\eta_a(x),\eta_b(x))$ to approximate the activation function, where $\eta_a(x)$ and $\eta_b(x)$ represent linear functions. Consequently, the formula for ACON as shown in Equation (1).

$$\begin{aligned} f_{ACON}(x) &= S_\beta(\eta_a(x),\eta_b(x)) \\ &= (\eta_a(x)-\eta_b(x))\cdot\sigma[\beta(\eta_a(x)-\eta_b(x))]+\eta_b(x) \end{aligned} \tag{1}$$

where σ represents the Sigmoid function. In this paper, ACON-C is employed as the improved activation function, which adaptively controls neuron weights using the same binary function. Let $\eta_a(x)=p_1x$, $\eta_b(x)=p_2x(p_1\neq p_2)$, mathematically, then the computation formula for ACON-C is provided in Equation (2) as follows:

$$\begin{aligned} f_{ACON-C}(x) &= S_\beta(p_1x,p_2x) \\ &= (p_1-p_2)x\cdot\sigma[\beta(p_1-p_2)x]+p_2x \end{aligned} \tag{2}$$

Meta-ACON employs a pre-designed neural network to determine the value of β, as depicted in Fig. 2. In order to demonstrate the dynamic nonlinearity of Meta-ACON, using $p_1=1.5$, $p_2=-0.5$ as an example, the Meta-ACON-C activation function is constructed. As the value of β changes, Meta-ACON-C dynamically transitions between non-linear and linear modes, as illustrated in Fig. 3. When $\beta\to\infty$, $f_{Meta-ACON-C}(x)\to\max(p_1x,p_2x)=1.5x$; when $\beta\to0$, $f_{Meta-ACON-C}(x)\to mean(p_1x,p_2x)=0.5x$.

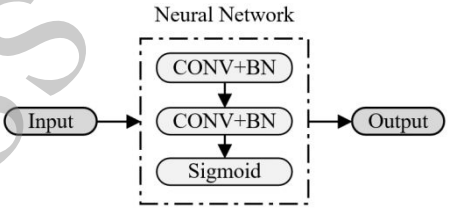

Fig. 2 Schematic diagram of Meta-ACON in non-linear and linear switching

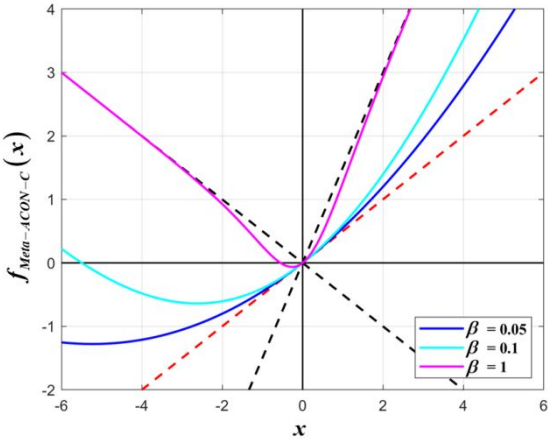

Fig. 3 Structure of the neural network for learning the switching factor

2.4 DnCNN-RM

This chapter is dedicated to the task of restoring a clean, noise-free image x from noisy observations $y=x+v$. Generally, v present in the images is modeled as additive white Gaussian noise (AWGN) with a standard deviation denoted by σ. In

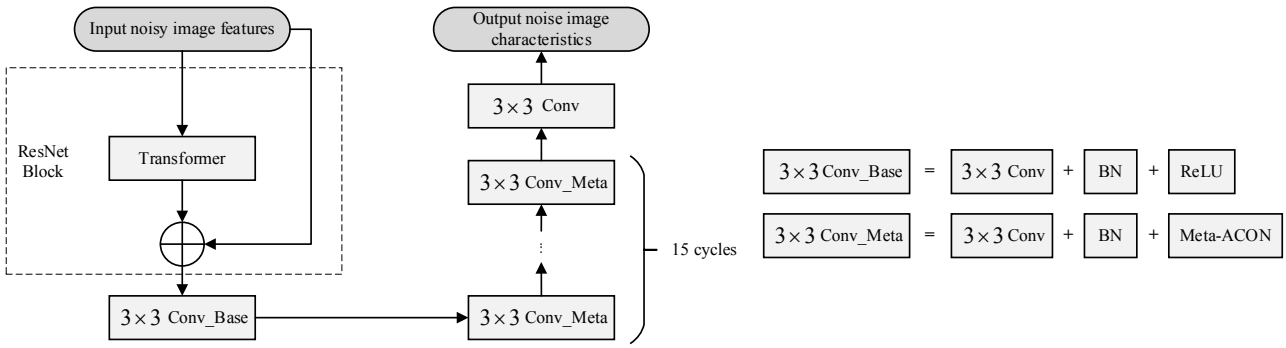

Fig. 4 DnCNN-RM network structure diagram

contrast to traditional denoising algorithms that rely on learning image priors to distinguish noise, DnCNN utilizes a neural network to effectively separate noise from the original image. The proposed DnCNN-RM framework is built upon DnCNN as the baseline, and its architecture is illustrated in Figure 4. This framework consists of 19 convolutional layers, each with unique parameter settings and structural configurations. In addition to incorporating a Transformer in the ResNet block, the kernel size for all subsequent layers is fixed. The stride for each layer is set to 1, and edge zero padding with a padding value of 0 is applied to the feature maps. These parameter configurations ensure that the intermediate layers of the network maintain consistent input and output dimensions. Furthermore, the use of edge zero padding helps prevent the introduction of boundary artifacts and the generation of redundant information, thereby preserving the quality of the image. To enhance feature extraction, this study employs the adaptive activation function Meta-ACON in the convolutional layers over 15 cycles, which improves the network's ability to capture critical features.

The input to DnCNN-RM consists of noisy image features denoted as $y = x + v$. DnCNN-RM takes a different approach by training residual mappings (denoted as $R(y) \approx v$). After training, the model outputs residual mappings that approximate the noise, and subsequently recovers clean, noise-free image features (denoted as $x = y - R(y)$) by subtracting the residual mappings from the original features. Formally, DnCNN-RM calculates the average mean square error (MSE) between the residual image and the noisy input, as shown in Equation (3):

$$\xi(\theta) = \frac{1}{2N}\sum_{i=1}^{N} \| R(y_i;\theta) - (y_i - x_i) \|_F^2 \tag{3}$$

where DnCNN-RM learns the training parameters θ by continuously iteratively updating the loss function $\xi(\theta)$, $\{(y_i, x_i)\}_{i=1}^{N}$ denoting the group of noisy clean training image pairs.

To maintain consistent input and output sizes and facilitate noise filtering through subtraction operations, the DnCNN-RM model avoids the use of pooling layers, relying instead on convolutional layers, batch normalization (BN) layers, and nonlinear activation layers. Specifically, the model includes the following four types of network layers:

(1) **Transformer-Based Residual Block:** In the residual block, we replace the convolutional neural network with a Transformer, which is more effective at extracting global information, to perform initial and comprehensive feature extraction. The Transformer module primarily consists of an encoder and a decoder, which work collaboratively to process global data.

(2) **Conv+Meta-ACON:** The layer employs a convolutional kernel of size 4 to generate feature maps, followed by the Meta-ACON activation function. This function enhances the network's ability to extract meaningful features by selectively activating neurons with useful information, while preserving the network's nonlinearity.

(3) **Conv:** In this layer, only convolutional kernels are used to generate the final output feature maps.

By integrating batch normalization, DnCNN-RM optimizes the network architecture, accelerating training and improving denoising performance. The model combines convolution with

the Meta-ACON activation function, allowing it to effectively separate clean images from noisy observations through hidden layers, extracting pure noise features directly. DnCNN-RM trains the network in an end-to-end manner and introduces a Transformer-Based residual mechanism module that learns to map noisy input images to their noise components, ultimately producing clean, noise-free images.

3 Experiments

3.1 Datasets

This paper experimentally validates the denoising performance of the DnCNN-RM algorithm using a dataset composed of real SAR images. These SAR images serve to evaluate the denoising effectiveness of the DnCNN-RM algorithm on real-world data, allowing for subsequent calculation of evaluation metrics and comparisons with other denoising algorithms. For model training, the Train400 and RSOD datasets are employed. The Train400 dataset comprises 400 clean, noise-free grayscale images, while the RSOD dataset includes 976 annotated images, all acquired through infrared sensors. After acquiring the images via infrared sensors, a deblurring process is applied to achieve an image resolution of 0.08 m, leading to the generation of the Vaihingen dataset. The infrared sensor system primarily consists of an array of infrared detectors and signal processing readout circuits. We use the general SAR dataset MSTAR to test the generalization ability of the proposed algorithm, demonstrating its practicality and high performance in the field of SAR denoising.

Due to the unique nature of coherent speckle noise, it is impossible to obtain a noise-free SAR image. Therefore, we simulate coherent speckle noise by using additive Gaussian noise. The noisy image is generated by adding the Gaussian noise to a clean image, and this noisy image is paired with the clean image to form a training dataset for training the network.

Before training, a preprocessing step is performed to introduce multiplicative noise to the clean images. Since the Train400 dataset consists of noise-free images that cannot directly simulate SAR data, multiplicative noise with a mean of 0 and a variance of 2 is randomly added to the original images. This noise closely mimics the coherent speckle noise typically observed in SAR images.

3.2 Experimental results and analysis

To verify the superiority and effectiveness of the DnCNN-RM algorithm, Fig. 5 and Fig. 6 present representative denoising results of various methods by using real SAR images (SAR1 and SAR2). Two sets of pictures are used to test the denoising performance of the algorithm for real SAR images. In this chapter, Lee's algorithm, Frost's algorithm, SAR-BM3D algorithm and DnCNN algorithm as the base model are used as comparison algorithms with DnCNN-RM algorithm to prove the excellent denoising effect of DnCNN-RM. During the training of DnCNN and DnCNN-RM, the learning rate is set to 0.001, the batch size is 128, and the number of iterations is set to 20.

Fig. 5 and Fig. 6 present the denoised image results of the five denoising algorithms for the real SAR images SAR1 and SAR2, respectively. The sub-images are described in detail, where Fig. (a) are all real SAR images, and Fig. (a) is input to each model as the input image to obtain the subsequent output results; Fig. (b) is the result graph using Lee's algorithm; Fig. (c) is the result graph of output denoising using Frost's algorithm; Fig. (d) is the result graph of denoising by SAR-BM3D algorithm; Fig. (e) shows the result graph after denoising by original model DnCNN algorithm. Fig. (f) is the result graph of output denoising using DnCNN-RM.

Table 1 and Table 2 present the denoising outcomes of six different algorithms applied to SAR1 and SAR2 images, alongside the corresponding evaluation indices of the original images. Given that synthetic aperture radar (SAR) inherently carries coherent speckle noise, achieving a completely noise-free and distortion-free SAR image is not feasible. To address this inherent limitation, this study incorporates the Equivalent Number of Looks (ENL) as an additional evaluation metric to more effectively assess the denoising performance of each algorithm.

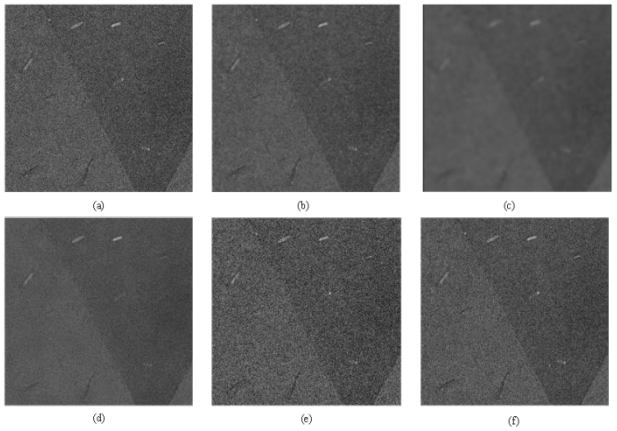

Fig. 5 The denoising results of SAR1 by different denoising algorithms

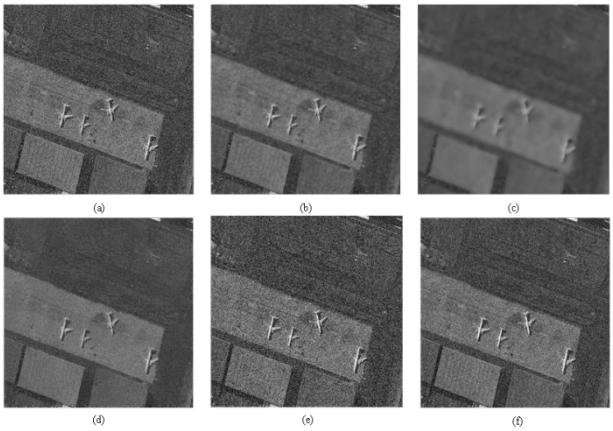

Fig. 6 The denoising results of SAR2 by different denoising algorithms

The results of the objective evaluation indices, shown in Table 1 and Table 2, highlight the comparative performance of the six denoising algorithms on the SAR1 and SAR2 images. For the SAR1 image, while maintaining excellent performance in EPI, SSIM, and ENL metrics, the PSNR reached a maximum of 59.011, demonstrating the superiority of the denoising process. For the SAR2 image, the PSNR improved nearly twofold compared to traditional algorithms, reaching 39.78. The experimental findings demonstrate that the DnCNN-RM algorithm achieves significantly superior denoising performance on real SAR images compared to traditional denoising methods.

Based on the experimental results, it can be concluded that the DnCNN-RM algorithm exhibits the most effective denoising performance on SAR images. This algorithm not only addresses the limitations of traditional denoising methods, which often rely heavily on filter design, but also enhances the denoising process by training specialized networks tailored to different noise types.

We conducted an ablation study on the DnCNN-RM model using the MSTAR dataset, comparing the denoising performance of several variants: DnCNN (Baseline), DnCNN + ResNet Block (CNN), DnCNN + ResNet Block (Transformer), and DnCNN + Meta-ACON. The experimental results are shown in Table 3.

Table 1. Denoising results of SAR1 by different SAR image denoising algorithms

Method	Mean	Std	PNSR	EPI	SSIM	ENL
Lee	118.44	13.73	14.74	0.987	0.996	0.999
Frost	115.32	10.74	12.49	0.833	0.979	0.999
SAR-BM3D	292.84	17.11	51.74	0.992	0.992	0.999
DnCNN	607.76	25.38	22.56	1.000	0.988	0.999
DnCNN-RM	697.12	25.22	**59.011**	1.000	0.999	0.999

Table 2. Denoising results of SAR2 by different SAR image denoising algorithms

Method	Mean	Std	PNSR	EPI	SSIM	ENL
Lee	556.73	23.38	18.38	0.989	0.995	0.999
Frost	409.82	20.24	24.55	0.735	0.978	0.999
SAR-BM3D	595.95	24.41	21.45	1.000	0.997	0.999
DnCNN	1180.49	34.36	23.40	1.000	0.987	0.999
DnCNN-RM	1150.26	35.65	**39.78**	0.999	0.999	0.999

Table 3. Denoising results of various denoising algorithms in ablation study

Method	PSNR
DnCNN	15.5135
DnCNN+ ResNet Block (CNN)	24.5698
DnCNN + ResNet Block (Transformer)	24.8080
DnCNN + Meta-ACON	24.5833
DnCNN+ ResNet Block (CNN) + Meta-ACON	24.5888
DnCNN + ResNet Block (Transformer) + Meta-ACON	**25.2021**

Table 4. Comparison results of SAR image denoising with different algorithms

Method	Wang et al. [14]	Zhang et al. [15]	Wang [16]	Ours
PSNR	22.7	22.44	22.90	**25.201**
SSIM	0.709	0.900	0.909	**0.951**

The experiments demonstrate that the Transformer-based residual block outperforms the CNN-based residual block in terms of global feature extraction capability, leading to improved removal of coherent speckle noise in SAR images. Both the Transformer-based ResNet Block (24.8080) and Meta-ACON (24.5833) provide a positive performance boost to the DnCNN model. Additionally, the strong compatibility between these two modules enables the final DnCNN-RM model (25.2021) to achieve the best overall performance.

The proposed DNCNN-RM algorithm was evaluated through comparative experiments with other commonly used SAR image denoising methods [14, 15, 16] under the same experimental conditions. The MSTAR dataset was employed for the evaluation, and the detailed results are presented in Table 4. The experimental results demonstrate that DNCNN-RM outperforms all the compared algorithms. Specifically, DNCNN-RM significantly surpasses the other methods in both PSNR and SSIM metrics, indicating its superior performance in denoising and preserving image details. Compared to other methods, DNCNN-RM is able to maintain higher image quality at higher noise levels, further enhancing denoising performance and detail retention. In conclusion, DNCNN-RM exhibits significant advantages in SAR image denoising tasks, effectively improving denoising results while preserving more image details, making it particularly suitable for SAR image processing in complex environments.

4 Conclusion

This paper addresses the challenge of denoising preprocessing for SAR images in complex electromagnetic environments. We propose a novel denoising algorithm, DnCNN-RM, which is built upon a deep learning framework and incorporates residual network modules. To enhance edge and texture preservation while mitigating the difficulty of training, we introduce residual units that refine the mapping between input and output within the DnCNN architecture. Additionally, we integrate the adaptive activation function Meta-ACON into the network, improving feature extraction capabilities while maintaining a lightweight network design.

References:

[1] THEODOSIOU A., LÓPEZ-DEKKER P., et al. On the sensitivity to height and motion of bistatic SAR interferometry: A spectral view[J]. IEEE Transactions on Geoscience and Remote Sensing, 2024, 62: 5212212.

[2] WU Y., et al. FAIR-CSAR: A Benchmark Dataset for Fine-Grained Object Detection and Recognition Based on Single-Look Complex SAR Images[J]. IEEE Transactions on Geoscience and Remote Sensing, 2025, 63: 5201022.

[3] ZHAO C., LI K., WANG L., OHTSUKI T., ADACHI F. A Rapid SAR Image Simulation Method for Ship Wakes Coupled With Sea Waves Using Fluid Velocity Potential[J]. IEEE Signal Processing Letters, 2025, 32: 271-275.

[4] GOU S., LI D., HAI D., et al. Spectral clustering with eigenvalue similarity metric method for POL-SAR image

segmentation of land cover[J]. Geographic Information Science, 2018.

[5] PETTINATO S., SANTI E., PALOSCIA S., et al. Large area robust identification of snow cover from multitemporal COSMO-SkyMed images[C]. Conference on SAR Image Analysis, Modeling, and Techniques, 2015.

[6] LI C., et al. Fast forest fire detection and segmentation application for UAV-assisted mobile edge computing system[J]. IEEE Internet of Things Journal, 2024, 11(16): 26690-26699.

[7] QIN C., ZHANG L., WANG X., LI G., HE Y., LIU Y. RDB-DINO: An Improved End-to-End Transformer With Refined De-Noising and Boxes for Small-Scale Ship Detection in SAR Images[J]. IEEE Transactions on Geoscience and Remote Sensing, 2025, 63: 5200517.

[8] JOSHI G P., ALENEZI F., THIRUMOOTHY G., et al. Ensemble of deep learning-based multimodal remote sensing image classification model on unmanned aerial vehicle networks[J]. Mathematics, 2021, 9(22): 2984.

[9] SUN Y., FENG S., YE Y., et al. Multisensor fusion and explicit semantic preserving-based deep hashing for cross-modal remote sensing image retrieval[J]. IEEE Transactions on Geoscience and Remote Sensing, 2021, 60: 1-14.

[10] THAKUR R S., YADAV R N., GUPTA L. State‐of‐art analysis of image denoising methods using convolutional neural networks[J]. IET Image Processing, 2019, 13(13): 2367-2380.

[11] DUAN Y., TAO X., HAN C., et al. Multi-scale convolutional neural network for SAR image semantic segmentation[C]. 2018 IEEE Global Communications Conference (GLOBECOM), 2018: 1-6.

[12] WANG C., YIN Z., MA X., et al. SAR image despeckling based on block-matching and noise-referenced deep learning method[J]. Remote Sensing, 2022, 14(4): 931-931.

[13] GUO Q., LIU J., KALIUZHNYI M. YOLOX-SAR: High-Precision object detection system based on visible and infrared sensors for SAR remote sensing[J]. IEEE Sensors Journal, 2022, 22(17): 17243-17253.

[14] WANG P., ZHANG H., PATEL V., et al. SAR image despeckling using a convolutional neural network[J]. IEEE Signal Processing Letters, 2017, 24(12): 1763-1767.

[15] ZHANG Q., YUAN Q., LI J., et al. Learning a dilated residual network for SAR image despeckling[J]. Remote Sensing, 2018, 10(2): 196-196.

[16] WANG X. Research on SAR Image Target Recognition Method Based on Deep Learning [D]. Chengdu: University of Electronic Science and Technology of China, 2023.

作者简介:

欧海宁（1979-），男，福建省莆田人，本科学士，2002 年于华侨大学获得学士学位。现就职于湄洲湾职业技术学院，主要从事自动化与机器视觉研究。E-mail：mzyxqb@126.com

曾瑞彬（1994-），男，福建宁德人，硕士研究生，2023 年于中国科学院大学获得硕士学位。现就职于湄洲湾职业技术学院，主要从事人工智能研究。E-mail：zengruibin19@mails.ucas.ac.cn